Semi-Analytical Modeling of Microring Resonators with Distributed Bragg Reflectors

Young Mo Kang and Lynford L. Goddard
University of Illinois at Urbana-Champaign
lgoddard@illinois.edu

***Abstract*-A semi-analytical method for fast simulation of microring resonators with distributed Bragg reflectors (DBR-MRR) is presented. Under the low loss condition, the structure exhibits a spectral response similar to that of a sampled-grating distributed Bragg reflector (SGDBR). However, the DBR-MRR can achieve higher reflectivity with significantly fewer gratings due to multiple reflection encounters with the same DBR gratings.**

I. Introduction

Microring resonators (MRR) have become essential building blocks in photonic integrated systems, serving as filters, modulators, laser cavities, sensors, and switches. Their compact sizes and flexibility in design and function have led to active research in different configurations including multiple rings, cascaded in series [1] and parallel [2], 2D arrayed [3], embedded [4], and spiral shape geometry [5]. In this paper, we focus on MRRs containing DBR gratings for the application of compact reflectors for tunable laser cavities [6].

II. Analysis

In the analysis, we separate the structure into two parts: the ring and the DBR. The microring part of the structure has been extensively studied and is well understood [7]. Likewise, the DBR part also has been extensively investigated and analyzed [8]. We thus combine the two results to obtain the characteristics of the whole structure.

We first use a black box model to represent the DBR in the ring. For simplicity in the analysis, we insert the black box at the center of the ring. Analysis for structures with the black box at different positions would proceed very similarly. Fig. 1 shows a simplified model to be used in the analysis. The black box inputs and outputs are related by the scattering matrix S_{BB},

$$\begin{bmatrix} out1 \\ out2 \end{bmatrix} = S_{BB} \begin{bmatrix} in1 \\ in2 \end{bmatrix} = \begin{bmatrix} \sigma_{11} & \sigma_{12} \\ \sigma_{21} & \sigma_{22} \end{bmatrix} \begin{bmatrix} in1 \\ in2 \end{bmatrix}. \quad (1)$$

At the waveguide-ring interface, we have a coupling matrix [9],

$$K = \begin{bmatrix} \tau & jk \\ jk & \tau \end{bmatrix} \quad (2)$$

where k and τ are coupling and transmission coefficients, respectively and $k^2 + \tau^2 = 1$ for lossless coupling. Since the fields will

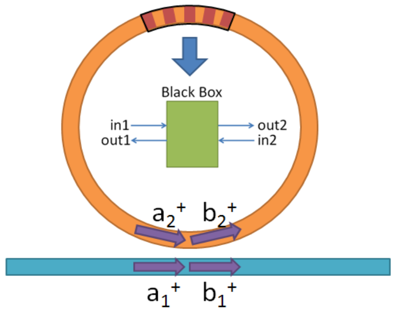

Fig. 1. Representing the DBR as a black box simplifies the analysis. The scattering matrix S_{BB} relates the two inputs to the two outputs. A racetrack geometry may be used to simplify the fabrication processes for the straight DBR gratings.

propagate in both counterclockwise and clockwise directions in the structure, we will use superscripts + and − to indicate fields propagating in these directions respectively. With this convention and the fields named in Fig. 1, we obtain two matrix equations describing the coupling,

$$\begin{bmatrix} {b_1}^+ \\ {b_2}^+ \end{bmatrix} = K \begin{bmatrix} {a_1}^+ \\ {a_2}^+ \end{bmatrix} \quad (3)$$

$$\begin{bmatrix} {a_1}^- \\ {a_2}^- \end{bmatrix} = K \begin{bmatrix} {b_1}^- \\ {b_2}^- \end{bmatrix}. \quad (4)$$

The inputs to the black box will be:

$$in1 = \alpha_r^{\frac{1}{2}} e^{j\frac{\theta_r}{2}} {a_2}^- \quad (5)$$

$$in2 = \alpha_r^{\frac{1}{2}} e^{j\frac{\theta_r}{2}} {b_2}^+ \quad (6)$$

where $\alpha_r = e^{-\frac{\rho}{2}L}$ is the optical field loss in one-round-trip in the ring excluding the black box. ρ is the optical loss coefficient, L is the circumference of the ring in the absence of the black box, and $\theta_r = \beta_r L = \frac{2\pi n_1 L}{\lambda}$ is the one-round-trip phase change in the ring where n_1 is the refractive index of the ring. Propagating these results to the waveguide-ring interface, we obtain:

$$\begin{bmatrix} {a_2}^+ \\ {b_2}^- \end{bmatrix} = \alpha_r e^{j\theta_r} S_{BB} \begin{bmatrix} {a_2}^- \\ {b_2}^+ \end{bmatrix}. \quad (7)$$

978-1-4244-4180-8/09/$25.00 ©2009 IEEE

Thus, solving (3), (4), and (7) yields:

$$b_1^{\ +} = \frac{\tau - \alpha_r^{\ 2}\, det(S_{BB})\tau e^{j2\theta_r} - \alpha_r(\sigma_{12}k^2 + (\sigma_{12}+\sigma_{21})\tau^2)e^{j\theta_r}}{1-\alpha_r(\sigma_{12}+\sigma_{21})\tau e^{j\theta_r} - \alpha_r^{\ 2}\, det(S_{BB})\tau^2 e^{j2\theta_r}} \quad (8)$$

$$a_1^{\ -} = \frac{-\alpha_r \sigma_{22} k^2 e^{j\theta_r}}{1-\alpha_r(\sigma_{12}+\sigma_{21})\tau e^{j\theta_r} - \alpha_r^{\ 2}\, det(S_{BB})\tau^2 e^{j2\theta_r}} \quad (9)$$

assuming $a_1^{\ +}$ is one and $b_1^{\ -}$ is zero.

The second part of the analysis will investigate the DBR's scattering matrix S_{BB}. The DBR structure consists of multiple pairs of (n_1, n_2) alternating material. We have defined the black box such that it is a symmetric structure and its outermost refractive index is n_2, as depicted in Fig. 2. One pair of grating can be seen as a (n_1, n_2, n_1) Fabry-Pérot (FP) resonator with extended material of refractive index n_1 at the right hand side. Using the scattering matrix of a FP resonator,

$$S_{FPR} = \begin{bmatrix} \frac{\Gamma(1-e^{j2\theta_2})}{1-\Gamma^2 e^{j2\theta_2}} & \frac{(1-\Gamma^2)e^{j\theta_2}}{1-\Gamma^2 e^{j2\theta_2}} \\ \frac{(1-\Gamma^2)e^{j\theta_2}}{1-\Gamma^2 e^{j2\theta_2}} & \frac{\Gamma(1-e^{j2\theta_2})}{1-\Gamma^2 e^{j2\theta_2}} \end{bmatrix} = \begin{bmatrix} r & t \\ t & r \end{bmatrix} \quad (10)$$

where $\Gamma = \frac{n_2-n_1}{n_1+n_2}$ and $\theta_i = \beta_i d_i = \frac{2\pi n_i d_i}{\lambda}$, we obtain the scattering matrix for a pair of lossless gratings:

$$S_{pair} = \begin{bmatrix} r & te^{j\theta_1} \\ te^{j\theta_1} & re^{j2\theta_1} \end{bmatrix}. \quad (11)$$

Using scattering and transmission matrices [8] to cascade these sub-blocks allows numerical calculation of S_{BB}. Substituting the elements of S_{BB} into (8) and (9) completely solves the spectral response of the DBR-MRR structure.

III. Simulation Results

Fig. 3a shows a simulation result of a DBR-MRR structure under the low loss condition of 1 *dB/cm* with only 10 pairs of (n_1, n_2) = (3, 3.01), (k^2, τ^2) = (0.1, 0.9), and the total ring circumference $Z_{DBR-MRR} = 15\frac{\lambda}{n} = 7.75\ \mu m$, for a design wavelength $\lambda = 1.55\ \mu m$. The spectral response of the DBR-MRR structure is similar to that of SGDBR as shown in Fig. 3b. The SGDBR has 45 sampled gratings, each of which is identical to the DBR of the DBR-MRR, but at a spatial sampling distance $Z_{SGDBR} = \frac{1}{2} Z_{DBR-MRR}$. This factor of 2 is introduced because the resonance of the DBR-MRR at very low $|\sigma_{11}|$ and $|\sigma_{22}|$ coincides with that of a simple MRR structure, i.e. when the circumference is an integer multiple of the effective wavelength. Using the DBR-MRR reduces the reflector length by more than 20 times, which thereby enables more compact and integrable structures.

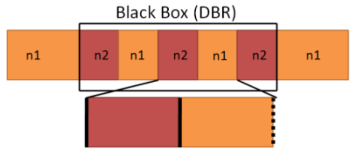

Fig. 2. The DBR consists of multiple pairs of n_1-n_2 alternations. Note that a pair consists of two index-interfaces (solid lines). The interface at the dashed line will be accounted for by the next pair or the rightmost FP resonator.

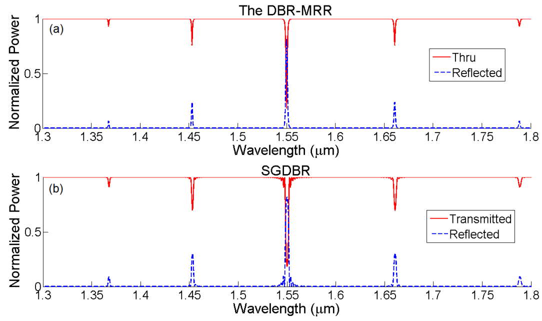

Fig. 3. Simulations of low loss structures. (a) DBR-MRR (b) SGDBR

IV. Conclusion

We presented a novel structure, the DBR-MRR, and a semi-analytical technique for fast simulation of its optical properties. The buildup of field strength in the ring resonator configuration enables the DBR-MRR to achieve high reflectivity with only a few pairs of low index contrast gratings.

Acknowledgment

The authors are grateful for startup fund support from the University of Illinois.

References

[1] J. E. Heebner, R. W. Boyd, and Q-H. Park, "SCISSOR solutions and other novel propagation effects in microresonator-modified waveguides," *J. Opt. Soc. Am. B*, **19**, pp. 722-731 (2002).

[2] A. M. Prabhu, H. L. Liew, and V. Van, "Generalized parallel-cascaded microring networks for spectral engineering applications," *J. Opt. Soc. Am. B*, **25**, pp. 1505-1514 (2008).

[3] Y. M. Ladobasa, S. Darmawan, and M.-K. Chin, "Matrix analysis of 2-D microresonator lattice optical fields," *IEEE J. Quantum Electron.*, **41**, pp. 1410-1418 (2005).

[4] L. Zhang, M. Song, T. Wu, L. Zou, R. G. Beausoleil, and A. E. Willner, "Embedded ring resonators for microphotonic applications," *Opt. Lett.*, **33**, pp. 1978-1980 (2008).

[5] D.-X. Xu, A. Densmore, A. Delâge, P. Waldron, R. McKinnon, S. Janz, J. Lapointe, G. Lopinski, T. Mischki, E. Post, P. Cheben, and J. H. Schmid, "Folded cavity SOI microring sensors for high sensitivity and real time measurement of biomolecular binding," *Opt. Exp.*, **16**, pp. 15137-15148 (2008).

[6] V. Jayaraman, Z.-M. Chuang, and L. A. Coldren, "Theory, design, and performance of extended tuning range semiconductor lasers with sampled gratings," *IEEE J. Quantum Electron.*, **29**, pp. 1824-1834 (1993).

[7] A. Yariv, "Universal relations for coupling of optical power between microresonators and dielectric waveguide," *Electron. Lett.*, **36**, pp. 321-322 (2000).

[8] L. A. Coldren and S. W. Corzine, *Diode lasers and photonic integrated circuits*, Wiley-Interscience, 1995.

[9] R. Grover, "Indium phosphide-based optical micro-ring resonators," Ph.D. thesis, Univ. of Maryland, College Park, MD, 2003 [online] Available: http://www.ece.umd.edu/research/microphotonics.